PHYSICAL REVIEW B **72**, 035216 (2005)

Theory of the spin EPR shift: Application to $\mathrm{Pb}_{1-x}\mathrm{Mn}_x\mathrm{Te}$

R. K. Das
Department of Physics, Gopalpur College, Gopalpur-on-sea, 761 002, Orissa, India

G. S. Tripathi*
Department of Physics, Berhampur University, Berhampur-760 007, Orissa, India

P. K. Misra
Department of Physics, Mesa State College, Grand Junction, Colorado 81502, USA
Department of Physics, University of Houston, Houston, Texas 77204, USA

(Received 20 October 2004; revised manuscript received 9 May 2005; published 18 July 2005)

We derive a theory for the spin-contribution to the electron-paramagnetic resonance shift (P_s) for an electronic system in the presence of a periodic potential, spin-orbit (SO) interaction, conduction electron-local moment interaction, and an applied magnetic field. An effective equation of motion of the Green's function is derived in the presence of the aforesaid interactions in a representation defined by the periodic part of the Bloch function. The spin-EPR shift is expressed as a function of the matrix elements of the momentum, Pauli spin-operators, and conduction electron-local moment interactions. We apply the theory to calculate P_s at Mn^{2+} ion in the diluted magnetic semiconductor (DMS) $\mathrm{Pb}_{1-x}\mathrm{Mn}_x\mathrm{Te}$, as a function of the carrier concentration. The electronic structure of the DMS is calculated using a modified six-level $\vec{k}\cdot\vec{\pi}$ ($\vec{\pi}$ is the momentum operator in the presence of SO interactions) model. Contributions from band-edge interactions as well as from far bands are included and relative strengths of these contributions are analyzed. P_s is found to be anisotropic arising due mainly to the SO interactions. Calculations of P_s for two typical hole densities agree fairly well with the experimental results for p-$\mathrm{Pb}_{1-x}\mathrm{Mn}_x\mathrm{Te}$. Discrepancies between theory and the experiment are analyzed.

DOI: 10.1103/PhysRevB.72.035216 PACS number(s): 75.50.Pp, 76.20.+q, 76.30.−v, 76.60.Cq

I. INTRODUCTION

The electron paramagnetic resonance (EPR) shift, which is a measure of an extra field (internal field) created at the magnetic ion site in magnetic materials or materials (metals and/or semiconductors) with magnetic impurities by the partial polarization of electrons and/or carriers in an applied magnetic field, constitutes an important study involving carriers and their interactions with the magnetic ions in an electronic system. The corresponding quantity in the nuclear magnetic resonance (NMR) is the Knight shift[1–3] which depends on the electron-nuclear hyperfine interaction. Both the studies furnish, in addition to ideas about the aforesaid interactions, important informations regarding the wave functions of the carriers and also the Fermi surface characteristics of the system.

Recently measurements of the EPR shift (mentioned as the EPR Knight shift) at Mn^{2+} site in diluted magnetic semiconductors such as PbMnTe and SnMnTe were reported.[4] While both n-type and p-type materials were considered for $\mathrm{Pb}_{1-x}\mathrm{Mn}_x\mathrm{Te}$ only p-type materials were considered for $\mathrm{Sn}_{1-x}\mathrm{Mn}_x\mathrm{Te}$; both for the compositions, $x=0.0003$ and 0.001. The EPR measurements were performed with a Brucker X-band spectrometer. Hall effect measurements were performed by a standard four probe dc technique. The systematics of the experimental observation are as follows: In case of $\mathrm{Pb}_{1-x}\mathrm{Mn}_x\mathrm{Te}$, measurements were performed for carrier concentrations ranging from $5\times10^{16}\ \mathrm{cm}^{-3}$ to about $2\times10^{19}\ \mathrm{cm}^{-3}$, for $x=0.0003$ and 0.001. The experimenters mentioned that they did not observe any appreciable difference in the shifts in the composition range considered. For p-$\mathrm{Pb}_{1-x}\mathrm{Mn}_x\mathrm{Te}$, the EPR shift is about -5.5×10^{-3} at $p=10^{17}\ \mathrm{cm}^{-3}$. With increase in the hole concentration, the shift increases and becomes positive at $p=10^{19}\ \mathrm{cm}^{-3}$. On the other hand, for the n-type material, the shift is about -4×10^{-3} at $n=10^{17}\ \mathrm{cm}^{-3}$ which decreases and becomes -11×10^{-3} at about $n=3\times10^{18}\ \mathrm{cm}^{-3}$. However for p-$\mathrm{Sn}_{1-x}\mathrm{Mn}_x\mathrm{Te}$, the range of carrier concentrations considered is approximately between $5\times10^{19}\ \mathrm{cm}^{-3}$ and $2\times10^{21}\ \mathrm{cm}^{-3}$; the range here corresponds to the carrier concentrations normally found in semimetals. The experimenters claim that theirs is the first observation of the EPR shift in the diluted magnetic semiconductors. They tried to interpret their results by using an empirical formula which is a function of the electron-magnetic ion interaction, the carrier g factor and the density of states at the Fermi surface.

We were motivated by these results because of our experience of working in the theoretical resonance phenomena, such as the Knight shift,[5–7] the chemical shift[8,9] and indirect nuclear spin-spin interactions[10,11] in one of the host systems, namely PbTe. We have recently done some theoretical investigations concerning the magnetization and electronic structure of the diluted magnetic superconductor (DMS) $\mathrm{Pb}_{1-x}\mathrm{Mn}_x\mathrm{Te}$[12,13] and the electronic structure of $\mathrm{Pb}_{1-x-y}\mathrm{Mn}_x\mathrm{Sn}_y\mathrm{Te}$.[14] The experimental results together with our aforesaid experience inspired us to pursue a rigorous theory of the observed phenomena. It may not be out of context to mention here that diluted magnetic semiconductors[15–21] in general and the aforesaid systems[22–24] in particular have attracted considerable attention due to the possibilities of carrier-mediated ferromagnetism in these systems, which could be of use in the emerging subject of spintronics. Thus research in the DMS has acquired immense current interest and importance.

In Sec. II, we derive a theory for the the spin contribution to EPR shift (denoted by the symbol P_s) in the presence of an applied magnetic field, spin-orbit interaction and electron-local magnetic moment interactions. The spin-orbit interaction is considered because these systems show large carrier g factors arising due mainly to this interaction. It may be noted that the g factors can also be affected by electron-local moment interactions.[25] However, we have not considered this effect in our theory. It is well known that magnetic vector potential destroys the lattice translational symmetry. However, this problem has been tackled by one of us previously in the derivation of the orbital magnetic susceptibility by using both Roth's function[26,27] and Green's function[28] and incorporating the Peierl's phase factor. We follow a Green's function approach here because of its inherent importance and popularity. The essential results of both the approaches are the same. The use of the Peierl's phase factor results in writing the effective equation of motion of the Green's function in a space defined by a magnetic wave vector, $\vec{\kappa}=\vec{k}+i\vec{h}\times\vec{\nabla}_k$, where $\vec{h}=e\vec{B}/\hbar c$ and $\vec{B}$ is the applied magnetic field. Interband effects are considered and P_s is obtained finally as a function of the matrix elements of the momentum operator, Pauli spin operators, the electron-local moment exchange operator and the density of states.

Section III describes the details of the application of the theory to p-Pb$_{1-x}$Mn$_x$Te, a diluted magnetic semiconductor based on the narrow gap lead salt, PbTe. We have chosen a p-type system because the valence band states transform like Pb s states which are relatively easier to handle than the conduction band states which transform like the Pb p orbitals. We have calculated P_s for two typical carrier (hole) densities, $p=5\times10^{17}$ cm^{-3} and $p=3\times10^{18}$ cm^{-3}. Experimental results are not available below the former value and our model shows certain inconsistencies above the latter value of the carrier density. We have calculated our values by considering three variants of the carrier electronic structure based on the $\vec{k}\cdot\vec{\pi}$ model.[29,30]

Section IV outlines the exchange interaction matrix elements which appear in the theory. The origin of the longitudinal and transverse contributions is also discussed in this section. Finally, we discuss our results followed by appropriate concluding remarks in Sec. V.

II. THEORY OF THE SPIN-EPR SHIFT

In this section we derive a theory of the spin-EPR shift. The shift corresponds to a change in the magnetic field ($\Delta\vec{B}$) experienced by magnetic ions in an electronic system due to partial polarization of conduction electrons in the presence of an applied magnetic field $\vec{B}$ and the electron-local moment (of the magnetic ion) interaction. For example, if the interaction of the local magnetic moment $\vec{M}$ of a magnetic ion in a diamagnetic environment is given by $\mathcal{H}_{\text{dia}}=-\vec{M}\cdot\vec{B}$, then the same interaction in a conduction-electron environment is given by

$$\mathcal{H} = -\vec{M}\cdot\vec{B}\left(1+\frac{\Delta\vec{B}}{\vec{B}}\right). \tag{1}$$

$\Delta\vec{B}/\vec{B}$ corresponds to the EPR shift, P. Since this shift is less than a few percent, the applied magnetic field and the electron-local moment interactions are considered as perturbations. We start, with the equation of motion of the one electron Green's function in the presence of the aforesaid interaction, the periodic potential and the spin-orbit interaction in the real space and derive an effective equation of motion for the same in the $\vec{k}$ space and separate the nonperturbing and perturbing parts of the Hamiltonian. Following Eq. (1) the EPR shift on the jth site is given by the expression

$$P_j^{\mu\nu} = -\left.\frac{\partial^2\Omega}{\partial B^\mu\partial M_j^\nu}\right|_{\vec{B}\to 0,\vec{M}_j\to 0}, \tag{2}$$

where Ω is the thermodynamic potential and is given by[31]

$$\Omega = -\frac{1}{\beta}\operatorname{Tr}\ln(-\mathcal{G}_{\xi_l}). \tag{3}$$

Tr involves summation over both imaginary frequencies and one-particle states forming a complete orthonormal set and $\mathcal{G}_{\xi_l}$ is the one-particle Greens function. The meaning of $\mathcal{G}_{\xi_l}$ would be clear in the following.

The one particle Green's function $G(\vec{r},\vec{r}\,',\vec{B},\vec{M}_j,\xi_l)$ in the presence of a periodic potential $V(\vec{r})$, spin-orbit interaction, applied magnetic field $\vec{B}$, and local magnetic moment at the jth site $\vec{M}_j$ satisfies the equation[32]

$$(\xi_l-\mathcal{H})G(\vec{r},\vec{r}\,',\vec{B},\vec{M}_j,\xi_l) = \delta(\vec{r}-\vec{r}\,'), \tag{4}$$

where ξ_l is the complex energy,

$$\xi_l = \frac{(2l+1)i\pi}{\beta}+\mu, \quad l=0,\pm 1,\pm 2,\ \ldots\ , \tag{5}$$

μ being the chemical potential and $\beta^{-1}=k_BT$. Further, the one-particle Hamiltonian is

$$\mathcal{H} = \frac{1}{2m}\left(\vec{p}+\frac{e}{c}\vec{A}\right)^2+V(\vec{r})+\frac{\hbar}{4m^2c^2}\vec{\sigma}\cdot\vec{\nabla}V\times\left(\vec{p}+\frac{e}{c}\vec{A}\right) + \frac{1}{2}g_0\mu_0\vec{B}\cdot\vec{\sigma}+\mathcal{H}_I, \tag{6}$$

where

$$\mathcal{H}_I = \frac{1}{2g_J\mu_0}\sum_j \vec{M}_j\cdot\vec{\sigma}\mathcal{J}(\vec{r}-\vec{R}_j). \tag{7}$$

In Eqs. (6) and (7), $\vec{A}$ is the magnetic vector potential, and $\mathcal{J}(\vec{r}-\vec{R}_j)$ is the strength of the exchange interaction between the conduction electron and the local moment at the jth site. Further g_j is the Lande g factor of the localized electron and μ_0 is the Bohr magneton. G satisfies the lattice translational symmetry in the absence of the applied magnetic field. However, this symmetry is destroyed by the magnetic field. In order to take care of this lack of lattice symmetry in the presence of the magnetic field, we express G as a product of the Green's function $\mathcal{G}$ which satisfies the lattice translational symmetry and the Peierl's phase factor[28] using the symmetric gauge for the vector potential value $\vec{A}(\vec{r})=\frac{1}{2}\vec{B}\times\vec{r}$,

$$G(\vec{r},\vec{r}',\vec{B},\vec{M}_j,\xi_l)=e^{i\vec{h}\cdot\vec{r}\times\vec{r}'}\mathcal{G}(\vec{r},\vec{r}',\vec{B},\vec{M}_j,\xi_l). \tag{8}$$

Here, as mentioned earlier,

$$\vec{h}=\frac{e\vec{B}}{2\hbar c}. \tag{9}$$

It would be pertinent here to comment on Eq. (8). The phase factor has the effect of translating the origin of the vector potential. The general Peierl's phase is $(e/2\hbar c)[A(\vec{r})+A(\vec{r}')]\cdot(\vec{r}-\vec{r}')$. The phase factor has been used by many authors.[33,34] It can be traced to Peierl's original paper.[35] However, recently there have been some attempts[36,37] to improve the treatment of Bloch electrons in a constant magnetic field beyond Peierl's approximation. A general theoretical approach for the nonperturbative Bloch solution of Schrödinger equation in the presence of a constant magnetic field is presented.[36] Using a singular gauge transformation based on a lattice of magnetic flux lines, an equivalent quantum system with a periodic vector potential is obtained. For rational magnetic field this system forms a magnetic superlattice for which Bloch's theorem then applies.

Derivation of the effective equation of motion by using Eq. (8) in Eq. (4) is quite complicated. However, this has been done in detail in an earlier work of one of the authors concerning the magnetic susceptibility of Bloch electrons.[28] Their effective equation of motion can be slightly modified to obtain the following:

$$[\xi_l-\mathcal{H}(\kappa)]\mathcal{G}(\vec{k},\xi_l)=I, \tag{10}$$

where

$$\mathcal{H}(\kappa)\approx\mathcal{H}_0(\vec{k})+\mathcal{H}'(\vec{k}). \tag{11}$$

These are given by

$$\mathcal{H}_0(\vec{k})=\frac{1}{2m}(\vec{p}+\hbar\vec{k})^2+V+\frac{\hbar}{4m^2c^2}\vec{\sigma}\cdot\vec{\nabla}V\times(\vec{p}+\hbar\vec{k}) \tag{12}$$

and

$$\mathcal{H}'(\vec{k})=-i\frac{\hbar}{m}h_{\alpha\beta}\pi^{\alpha}\nabla_k^{\beta}+\frac{1}{2}g_0\mu_0\sigma^{\mu}H^{\mu}+\frac{1}{2\mu_0}\sum_j\frac{1}{g_j}M_j^{\nu}\sigma^{\nu}\mathcal{J}. \tag{13}$$

Repeated indices here and elsewhere in the work imply summation over Cartesian components and κ, as mentioned earlier, is given by

$$\vec{\kappa}=\vec{k}+i\vec{h}\times\vec{\nabla}_k. \tag{14}$$

Equation (10) is derived in a representation defined by the periodic part $u_{\vec{k}\rho}(\vec{r})$ of the Bloch function $\psi_{\vec{k}\rho}$, where $\vec{k}$ is the reduced wave vector. Further

$$\vec{\pi}=\vec{p}+\frac{\hbar}{4mc^2}\vec{\sigma}\times\vec{\nabla}V, \tag{15}$$

momentum operator in the presence of the spin-orbit interaction and $h_{\alpha\beta}=\epsilon_{\alpha\beta\mu}h^{\mu}$. Here $\epsilon_{\alpha\beta\mu}$ is an antisymmetric tensor of third rank and we follow Einstein summation convention. Equation (3) can be further simplified by writing the frequency summation as

$$\Omega=-\frac{1}{2\pi i}\mathrm{tr}\oint_c\phi(\xi)\mathcal{G}(\xi)d\xi, \tag{16}$$

where

$$\phi(\xi)=-\frac{1}{\beta}\ln[1+e^{-\beta(\mu-\xi)}] \tag{17}$$

and tr involves summation over one particle states only. The contour c encircles the imaginary axis in an anticlockwise direction. Equation (10) can be solved by a perturbation expansion of $\mathcal{G}(\vec{k},\xi)$,

$$\begin{aligned}\mathcal{G}(\vec{k},\xi)&=\mathcal{G}_0(\vec{k},\xi)+\mathcal{G}_0(\vec{k},\xi)\mathcal{H}'\mathcal{G}_0(\vec{k},\xi)\\&\quad+\mathcal{G}_0(\vec{k},\xi)\mathcal{H}'\mathcal{G}_0(\vec{k},\xi)\mathcal{H}'\mathcal{G}_0(\vec{k},\xi).\end{aligned} \tag{18}$$

We have retained terms up to second order since we are interested in the EPR shift independent of the applied field and the local moment. In Eq. (18) $\mathcal{G}_0(\vec{k},\xi)$ satisfies the equation

$$[\xi-\mathcal{H}_0(\vec{k})]\mathcal{G}_0(\vec{k},\xi)=I \tag{19}$$

and is diagonal in the basis $u_{\vec{k}\rho}(\vec{r})$. The first two terms in Eq. (18) would not contribute to the EPR shift, and this could be easily tested from the inspection of Eq. (2). Using Eq. (18) and the identity[28]

$$\nabla_k^{\alpha}\mathcal{G}_0(\vec{k},\xi)=\frac{\hbar}{m}\mathcal{G}_0(\vec{k},\xi)\pi^{\alpha}\mathcal{G}_0(\vec{k},\xi), \tag{20}$$

we can write

$$\begin{aligned}\mathcal{G}(\vec{k},\xi)=\sum_j M_j^{\nu}B^{\mu}\frac{1}{2g_j}\Bigg(&(\mathcal{G}_0\sigma^{\mu}\mathcal{G}_0\sigma^{\nu}\mathcal{J}\mathcal{G}_0+\mathcal{G}_0\sigma^{\nu}\mathcal{J}\mathcal{G}_0\sigma^{\mu}\mathcal{G}_0)\\&-\frac{i}{m}\epsilon_{\alpha\beta\mu}(\mathcal{G}_0\pi^{\alpha}\mathcal{G}_0\pi^{\beta}\mathcal{G}_0\sigma^{\nu}\mathcal{J}\mathcal{G}_0\\&+\mathcal{G}_0\sigma^{\nu}\mathcal{J}\mathcal{G}_0\pi^{\alpha}\mathcal{G}_0\pi^{\beta}\mathcal{G}_0)\Bigg).\end{aligned} \tag{21}$$

Here $\mathcal{G}_0$ is the compact form of $\mathcal{G}_0(\vec{k},\xi)$. Equation (16) is evaluated using Eqs. (17) and (21). Denoting the contributions of the first and second terms of Eq. (21) to Ω as Ω_1 and Ω_2, we write

$$\Omega=\Omega_1+\Omega_2, \tag{22}$$

where

$$\Omega_1 = \sum_j H^{\mu} M_j^{\nu} \sum_{n\vec{k}\rho\rho'} \left(\frac{1}{2g_j}\sigma^{\nu}\mathcal{J}\right)_{n\rho,n\rho'} \sigma^{\mu}_{n\rho',n\rho} f'(E_{n\vec{k}\rho}) \tag{23}$$

and Ω_2 is obtained after a straightforward but little tedious evaluation as

$$\Omega_2 = \sum_j H^{\mu} M_j^{\nu} \sum_{n,m,\vec{k},\rho,\rho',\rho''_{m\neq n}} \times \frac{i}{m}\epsilon_{\alpha\beta\mu} \frac{\left(\frac{1}{2g_j}\sigma^{\nu}\mathcal{J}\right)_{n\rho,n\rho'} \pi^{\alpha}_{n\rho',m\rho''}\pi^{\beta}_{m\rho''n\rho}}{E_{mn}} f'(E_{n\vec{k}\rho}). \tag{24}$$

In Eqs. (23) and (24) $f'(E_{n\vec{k}})$ is the first derivative of the Fermi function and $E_{n\vec{k}}$ satisfies the equation

$$\mathcal{H}_0 u_{n\vec{k}\rho}(\vec{r}) = E_{n\vec{k}} u_{n\vec{k}\rho}(\vec{r}). \tag{25}$$

Ω_2 arises due to the spin-orbit interaction and is zero in the absence of it. This is a very important term in semiconductors with large spin-orbit interaction energy. The matrix elements of type $Q_{n\rho,n\rho'}$ are given by

$$Q_{n\rho,n\rho'} = \frac{(2\pi)^3}{\Omega_c}\int_{\text{cell}} u^{*}_{n\vec{k}\rho}(\vec{r}) Q u_{n\vec{k}\rho}(\vec{r}) d\vec{r}, \tag{26}$$

where Ω_c is the unit cell volume and

$$E_{mn} = E_m(\vec{k}) - E_n(\vec{k}). \tag{27}$$

From Eqs. (2) and (22)–(24) the spin contribution to the EPR shift at the jth site is given by

$$P^{\nu\mu}_{js} = -\sum_{n,\vec{k},\rho,\rho'\rho'',m\neq n} \frac{1}{2g_j}(\sigma^{\nu}\mathcal{J})_{n\rho,n\rho'} \left(\sigma^{\mu}_{n\rho',n\rho} + \frac{i}{m}\epsilon_{\alpha\beta\mu}\frac{\pi^{\alpha}_{n\rho',m\rho''}\pi^{\beta}_{m\rho'',n\rho}}{E_{mn}}\right) f'(E_{n\vec{k}}). \tag{28}$$

A more rigorous analysis would have yielded additional terms arising out of the effect of the spin-orbit interaction on the orbital motion of Bloch electrons. However, since we are interested only in the spin-contribution to the EPR shift, we have not considered these terms. Equation (28) can further be written in terms of the effective g factor as

$$P^{\nu\mu}_{js} = -\frac{1}{2}\sum_{n\vec{k}\rho\rho'} \left(\frac{1}{2g_j}\sigma^{\nu}\mathcal{J}\right)_{n\rho,n\rho'} g^{\mu}_{nn}(\vec{k})\sigma^{\mu}_{n\rho',n\rho} f'(E_{n\vec{k}}), \tag{29}$$

where the effective g factor $g^{\mu}_{nn}(\vec{k})$ is defined through the equation

$$g^{\mu}_{nn}(\vec{k})\sigma^{\mu}_{n\rho',n\rho} = g_0\sigma^{\mu}_{n\rho',n\rho} + \frac{2i}{m}\epsilon_{\alpha\beta\mu}\sum_{m\neq n,\rho''}\frac{\pi^{\alpha}_{n\rho',m\rho''}\pi^{\beta}_{m\rho'',n\rho}}{E_{mn}}. \tag{30}$$

Equation (29) can be applied to both metals and semiconductors with magnetic ions and appreciable spin-orbit interaction. In the following sections we have applied this formula to the calculation of the EPR shift at Mn^{2+} site in $\mathrm{Pb}_{1-x}\mathrm{Mn}_x\mathrm{Te}$. However, it can be expressed in a simplified way, if we make drastic approximations, by considering the quantities appearing on the right-hand side of Eq. (29), averaged over the Fermi surface, as

$$P_{js} = J_{jsd}\, g_{\text{eff}}\, \rho(\epsilon_F), \tag{31}$$

where

$$J_{jsd} = \left\langle \frac{1}{4g_j}\sigma^{z}\mathcal{J}\right\rangle_{\mathcal{F}}, \tag{32}$$

g_{eff} is the average value of the effective g factor evaluated at the Fermi surface and $\rho(\epsilon_F)$ is the density of states which is obtained by considering the fact that $-f'(\epsilon-\epsilon_F)=\delta(\epsilon-\epsilon_F)$. Equation (31) is the formula used for the experimental analysis.[4] However, in what follows, we shall use Eq. (28) for the evaluation of the spin-EPR shift. In order to do this we consider the carrier-concentration dependent electronic structure of $\mathrm{Pb}_{1-x}\mathrm{Mn}_x\mathrm{Te}$ in the following section.

III. ELECTRONIC STRUCTURE OF $\mathrm{Pb}_{1-x}\mathrm{Mn}_x\mathrm{Te}$

A. $\vec{k}\cdot\vec{\pi}$ model

We wish to calculate the electronic structure of $\mathrm{Pb}_{1-x}\mathrm{Mn}_x\mathrm{Te}$ using a $\vec{k}\cdot\vec{\pi}$ model and use it for the evaluation of the EPR shift. Details of this kind of calculation are presented in an earlier work[14] by two of the authors. We only reproduce a part of it which is essential to make the paper self-contained. Depending on the level of sophistication and the character of the particular problem at hand, one can use one-band or multiband Kohn-Luttinger[29] or Kane[30] model Hamiltonians. The principles of both the models are same. However, in the original Kohn-Luttinger effective mass representation, only interactions within the valence band are treated exactly; interactions with all other bands are considered using perturbation theory. However, in the Kane's model, both valence and conduction bands are treated exactly.

The method supposes that energy bands and wave functions have been determined by some process for a reference point in the Brillouin zone, $\vec{k}_0$. Then we ask for these quantities at a neighboring point $\vec{k}$. Let $\psi_n(\vec{k},\vec{r})$ be the wave function for a state in the nth band at position $\vec{k}$ in the zone, and let $\psi_j(\vec{k}_0,\vec{r})$ refer to the jth band at $\vec{k}_0$. It is convenient to define a set of functions[29]

$$\chi_j(\vec{k},\vec{r}) = e^{i(\vec{k}-\vec{k}_0)\cdot\vec{r}}\psi_j(\vec{k}_0,\vec{r}). \tag{33}$$

These functions form a complete orthonormal set. The unknown $\psi_n(\vec{k},\vec{r})$ is expanded in terms of the known functions χ_j,

$$\psi_n(\vec{k},\vec{r}) = \sum_j A_{nj}(\vec{k})\chi_j(\vec{k},\vec{r}), \tag{34}$$

where $A_{nj}(\vec{k})$ are the expansion coefficients. It may be noted that we cannot expand $\psi_n(\vec{k},\vec{r})$ directly in terms of $\psi_j(\vec{k}_0,\vec{r})$

since functions belonging to different wave vectors are orthogonal. Substituting Eq. (34) in the following eigenvalue equation,

$$\left(\frac{\pi^2}{2m}+U(\vec{r})\right)\psi_n(\vec{k},\vec{r})=E_n(\vec{k})\psi_n(\vec{k},\vec{r}), \qquad (35)$$

we obtain, following a straightforward but tedious process, the effective equation of motion:

$$\sum_j\left[\left(E_j(\vec{k}_0)-E_n(\vec{k})+\frac{\hbar^2}{2m}(k^2-k_0^2)\right)\delta_{jl}+\frac{\hbar}{m}(\vec{k}-\vec{k}_0)\cdot\vec{\pi}_{lj}\right]A_{nj}(\vec{k})=0 \qquad (36)$$

in which

$$\vec{\pi}_{lj}=\frac{(2\pi)^3}{\Omega_c}\int_{\text{cell}}d^3r\,u_l^*(\vec{k}_0,\vec{r})\vec{\pi}u_j(\vec{k}_0,\vec{r}). \qquad (37)$$

There is one equation for each value of the band index l. The index n (on A_{nj}) refers to the nth solution of the equations, and may be suppressed without leading to misunderstanding. The condition for this infinite set of simultaneous, linear, homogeneous equations to have a nontrivial solution is that the determinant of the coefficients should vanish. A general element of this determinant has the form

$$\mathcal{H}_{jl}-E(\vec{k})\delta_{jl} \qquad (38)$$

with

$$\mathcal{H}_{jl}=\left(E_j(\vec{k}_0)+\frac{\hbar^2}{2m}(k^2-k_0^2)\right)\delta_{jl}+\frac{\hbar}{m}(\vec{k}-\vec{k}_0)\cdot\vec{\pi}_{lj}. \qquad (39)$$

The problem is to diagonalize the effective Hamiltonian matrix, whose elements are given by Eq. (39).

Although this procedure has been developed with the intention that it will be used to relate energies of states at neighboring points of the zone, there is nothing in the derivation of the effective Hamiltonian which restricts us to this situation. If enough states are included in the Hamiltonian, there is no reason why the bands cannot be obtained throughout the zone. This supposes that there is enough experimental or theoretical information available from other sources to fix the values of the momentum matrix elements on which the calculation depends and which may be regarded as adjustable parameters. It may be mentioned, in passing, that a Taylor's expansion of $E(\vec{k}-\vec{k}_0)$ is also used for this purpose. However, this is not a popular method.

B. $\vec{k}\cdot\vec{\pi}$ model for PbTe

The host material PbTe is a narrow gap degenerate semiconductor with the minimum gap E_G occurring at the L point, $(2\pi/a)(\frac{1}{2},\frac{1}{2},\frac{1}{2})$ in the Brillouin zone. In addition to the band edge states, there are two more bands each above and below the minimum gap, which contribute to the $\vec{k}\cdot\vec{\pi}$ model[32,33] (Fig. 1). In the presence of the spin-orbit interaction, each band is Kramer's split and there are 12 states altogether. In the usual $\vec{k}\cdot\vec{\pi}$ approach[5] for lead salts, the Hamiltonians for the band edge states are diagonalized exactly and the far bands (both conduction and valence) are treated using second order perturbation theory, keeping terms up to k^4 in the energy expansion. We call this method the old model. This can still be extended to include terms up to k^6 as to be applicable at high carrier densities. This extension is termed as the old model plus sixth-order corrections to the energy. However, as we shall see later both these models do not work satisfactorily for our calculation.

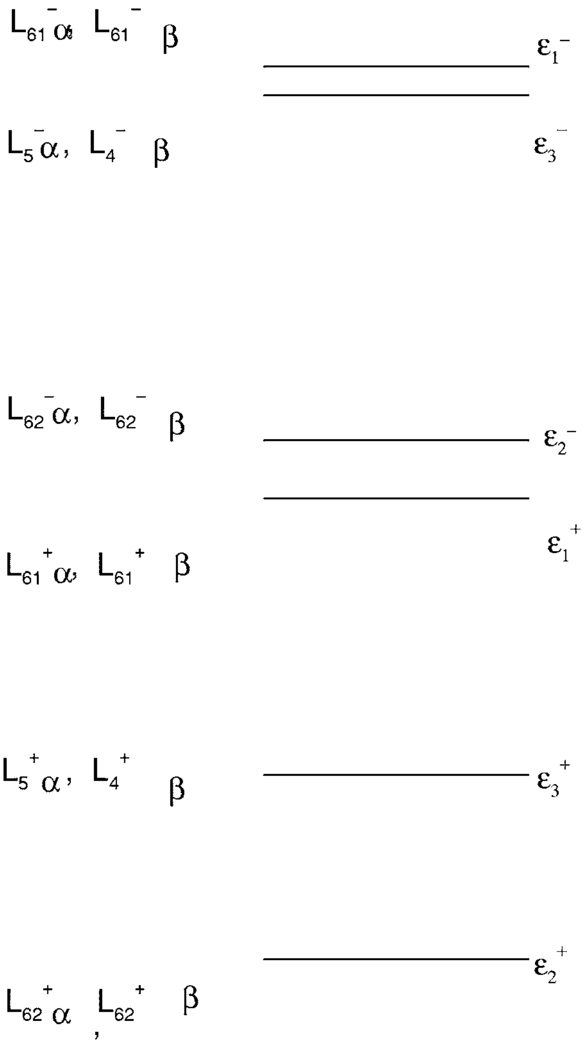

FIG. 1. Schematic picture of energy levels at the L point of the Brillouin zone in PbTe. The L-point double group basis functions are taken from Mitchell and Wallis (Ref. 32) and the ordering of bands is as per Bernick and Kleinman (Ref. 33).

Therefore, we consider an improvement as follows. Instead of diagonalizing the band edge Hamiltonians only, all the six bands could be diagonalized exactly through a 12×12 matrix. However, this must be done numerically. Although with the availability of modern computing facilities, this is no longer formidable; application of this model to our present theory involving matrix elements of momentum and $s(p)$-d hybridization operators would be enormously difficult. The other way is to follow a successive diagonalization of the band edge states. This is also formidable. Therefore, we have rediagonalized the band edge states by considering the energies and wave functions of the first diagonalization as the basis and treated the far bands, as usual, by perturbation theory. We have followed such an approach to calculate the Fermi energy and the density of states (DOS) as functions of carrier density for p-$\mathrm{Pb}_{1-x-y}\mathrm{Sn}_x\mathrm{Mn}_y\mathrm{Te}$ recently.[14]

The physical justification of this rediagonalization is that, although the first diagonalization is exact, the second diagonalization was necessitated because $\mathcal{H}' = (\hbar/m)\vec{k}\cdot\vec{\pi}$ ($\vec{k}_0$ is chosen as the origin of the calculation) is carrier concentration dependent and its strength increases as a function of this carrier density. With the change in the carrier density, the shape of the Fermi surface changes, resulting in the change of the Fermi momentum. This Fermi momentum is not borrowed from experiments, but obtained, by solving the dispersion relation self-consistently which in turn depends on the $\mathcal{H}'$. Thus there is an effective dependence of the carrier density on the accuracy of the treatment of $\mathcal{H}'$. This is called the new method.[14,38]

It may be noted that final results of this work are presented in a small paragraph of about dozen lines in Ref. 38. However, the focus there was on the carrier electronic structure calculation in the lead salts without magnetic ions. We reproduce some identical equations below from Refs. 14 and 38 to make the paper self-contained.

The diagonalization of the band edge Hamiltonians described by the Mitchell and Wallis (MW)[39] basis states and Bernick and Kleinman (BL)[40] ordering with the above $\mathcal{H}'$ give (ψ_1, ψ_2) for the conduction band and (ψ_3, ψ_4) for the valence band, and the corresponding energies are E_2^- and E_1^+. These are

$$\psi_1 = QL_{62}^-\alpha - Tk_zL_{61}^+\alpha + Sk_+L_{61}^+\beta, \tag{40}$$

$$\psi_2 = QL_{62}^-\beta + Tk_zL_{61}^+\beta + Sk_-L_{61}^+\alpha, \tag{41}$$

$$\psi_3 = QL_{61}^+\alpha + Tk_zL_{62}^-\alpha - Sk_+L_{62}^-\beta, \tag{42}$$

$$\psi_4 = QL_{61}^+\beta - Tk_zL_{62}^-\beta - Sk_-L_{62}^-\alpha, \tag{43}$$

and

$$E_2^- = \epsilon_2^- + \frac{\hbar^2k^2}{2m} + (1/2)E_G(W-1), \tag{44}$$

$$E_1^+ = \epsilon_1^+ + \frac{\hbar^2k^2}{2m} - (1/2)E_G(W-1), \tag{45}$$

where

$$Q = \left(\frac{1+W}{2W}\right)^{1/2}, \tag{46}$$

$$T = \frac{\sqrt{2}\frac{\hbar}{m}t}{E_G\sqrt{W(1+W)}}, \tag{47}$$

and

$$S = \frac{\sqrt{2}\frac{\hbar}{m}s}{E_G\sqrt{W(1+W)}}. \tag{48}$$

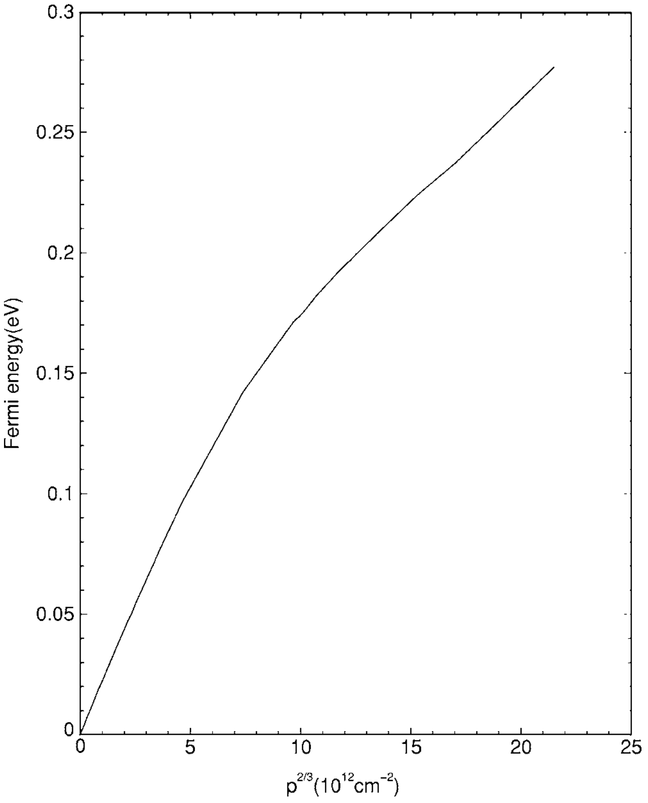

FIG. 2. The Fermi energy (in eV) is plotted as a function of hole concentration. $p^{2/3}$ is chosen for the abscissa because, for a free-carrier-type behavior, the curve should have been a straight line. Thus departure from the linear behavior suggests the manifestations of nonparabolicity of the energy bands and nonspherical Fermi surfaces.

$(L_{62}^-\alpha, L_{62}^-\beta)$ and $(L_{61}^+\alpha, L_{61}^+\beta)$ are the basis functions for the conduction and the valence band-edge states in the MW notation.[39] α and β denote the Kramer's conjugate pairs. The other symbols are

$$s = \langle L_{61}^+\alpha|\pi^+|L_{62}^-\beta\rangle = \langle L_{61}^+\beta|\pi^-|L_{62}^-\alpha\rangle, \tag{49}$$

$$t = -\langle L_{61}^+\alpha|\pi^z|L_{62}^-\alpha\rangle = \langle L_{61}^+\beta|\pi^z|L_{62}^-\beta\rangle, \tag{50}$$

$$k_\pm = \frac{(k_x \pm ik_y)}{\sqrt{2}}, \tag{51}$$

$$\pi^\pm = \frac{(\pi^x \pm i\pi^y)}{\sqrt{2}}, \tag{52}$$

$$W = \sqrt{1 + \alpha k_\rho^2 + \beta k_z^2}, \tag{53}$$

$$\alpha = 2\frac{\hbar^2}{m^2}\frac{s^2}{E_G^2}, \tag{54}$$

$$\beta = 4\frac{\hbar^2}{m^2}\frac{t^2}{E_G^2}, \tag{55}$$

and

$$k_\rho^2 = k_x^2 + k_y^2. \tag{56}$$

ϵ_2^- and ϵ_1^+ are the conduction and valence band energies at the L point which is considered as the origin of the $\vec{k}$ space. As mentioned earlier, we have rediagonalized the Hamiltonian considering Eqs. (40)–(43) as the basis wave functions and Eqs. (44) and (45) as the corresponding energies. After rediagonalization, we obtain

$$\phi_1 = X_\eta \psi_1 + X_\delta \psi_3 + X_\gamma \psi_4, \tag{57}$$

$$\phi_2 = X_\eta \psi_2 + X_\gamma \psi_3 - X_\delta \psi_4, \tag{58}$$

$$\phi_3 = X_\eta \psi_3 - X_\delta \psi_1 - X_\gamma \psi_2, \tag{59}$$

and

$$\phi_4 = X_\eta \psi_4 - X_\gamma \psi_1 + X_\delta \psi_2. \tag{60}$$

The new conduction band and valence band energies are

$$\mathcal{E}_2^- = E_2^- + (1/2)E_G W(X-1) \tag{61}$$

and

$$\mathcal{E}_1^+ = E_1^+ - (1/2)E_G W(X-1). \tag{62}$$

The symbols used are

$$X = \sqrt{(1+\eta)^2 + \delta^2 + \gamma^2}, \tag{63}$$

$$\eta = \frac{2P_{11}}{E_G W}, \tag{64}$$

$$\delta = \frac{2P_{13}}{E_G W}, \tag{65}$$

$$\gamma^2 = \frac{4|P_{14}|^2}{E_G^2 W^2}, \tag{66}$$

$$X_\eta = \sqrt{\frac{1+X+\eta}{2X}}, \tag{67}$$

$$X_\delta = \frac{\delta}{\sqrt{2X(1+X+\eta)}}, \tag{68}$$

and

$$X_\gamma = \frac{\gamma}{\sqrt{2X(1+X+\eta)}}. \tag{69}$$

P_{11}, P_{13}, and P_{14} are single group momentum matrix elements and are defined in Ref. 39. The total energy for both the conduction and the valence bands can be obtained by treating the far bands using perturbation theory. The evaluation of this energy, the Fermi energy and the density of states is given in detail in Ref. 14. In the limits of η, δ, and γ going to zero, our new method reduces to our old method. The band gap as a function of Mn concentration x is given by[41]

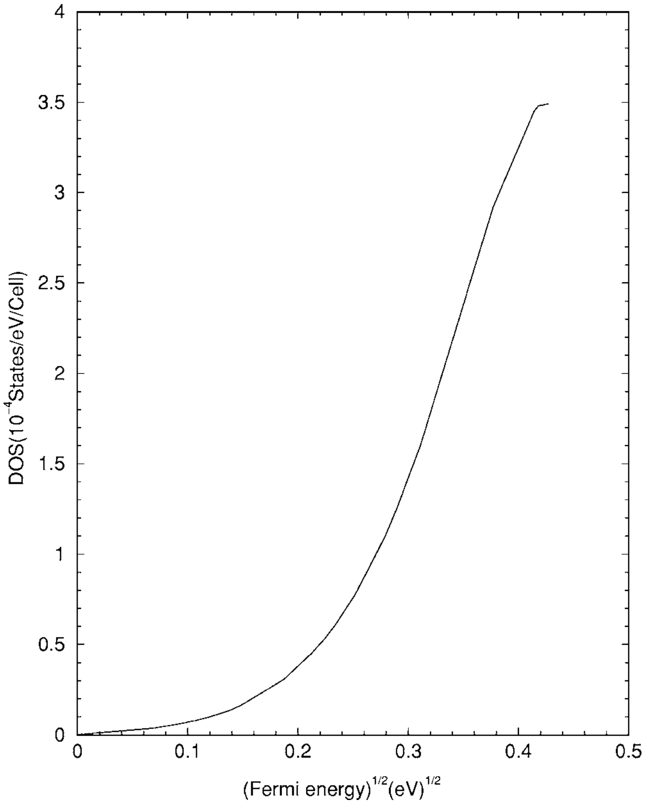

FIG. 3. The density of states is plotted as a function of the square root of the Fermi energy. For parabolic bands, this should have been linear. Departure from the linearity implies that the bands are nonparabolic and Fermi surfaces nonspherical.

$$E_G(x) = E_G(0) + 2.51x. \tag{70}$$

In Figs. 2 and 3, we plot the Fermi energy versus $p^{2/3}$ where p is the hole concentration and the density of states (DOS) vs $(\epsilon_{F_p})^{1/2}$, respectively. In Fig. 2, the abscissa is chosen as $p^{2/3}$ instead of p because the Fermi energy is linear in $p^{2/3}$. Deviation from the linear behavior suggests nonparabolic energy bands and nonspherical Fermi surfaces. Figure 3 also reveals the same kind of deviation from linearity for the DOS as a function of $\epsilon_F^{1/2}$. Similar behavior was observed in p-$\mathrm{Pb}_{1-x-y}\mathrm{Sn}_x\mathrm{Mn}_y\mathrm{Te}$ as well.[14]

IV. EPR SHIFT IN p-$\mathrm{Pb}_{1-x}\mathrm{Mn}_x\mathrm{Te}$

In the preceding sections we have discussed the theory of the EPR shift and the electronic structure of p-$\mathrm{Pb}_{1-x}\mathrm{Mn}_x\mathrm{Te}$ as a function of carrier density (in this case the hole concentration). We shall now consider both these aspects together and evaluate the EPR shift at the Mn^{2+} site in p-$\mathrm{Pb}_{1-x}\mathrm{Mn}_x\mathrm{Te}$ as a function of the hole concentration. The MW basis states for the band edge levels at the L point are[39]

$$L_{61}^+\alpha(\beta) = \mp i\cos\theta^+ R\uparrow(\downarrow)_{\mp}\sin\theta^+ S_\pm\downarrow(\uparrow), \tag{71}$$

and

TABLE I. Different contribution to P_s^l (all values in the units of 10^{-3}) at Mn^{2+} ion in $\mathrm{Pb}_{1-x}\mathrm{Mn}_x\mathrm{Te}$. Both two-band (band edge) and far-band contributions are considered. The far-band contributions together are opposite to the dominant two-band contributions. The far bands contribute about one-third of the two-band contribution. At higher carrier concentration the fraction of the far-band contributions increases further and is about one-half of the two-band contribution.

p (cm^{-3})	P_s^l (two-band)	P_s^l (far-band-inter)	P_s^l (far-band-intra)	P_s^l
5×10^{17}	−2.22	0.679	0.0257	−1.5
3×10^{18}	−1.98	0.905	0.071	−0.999

$$L_{62}^{-}\alpha(\beta) = \sin\theta^{-} Z\uparrow(\downarrow) \pm \cos\theta^{-} X_{\pm}\downarrow(\uparrow), \tag{72}$$

where R is an atomic s state around Pb, Z and $X_\pm$ are atomic p states with $m_z=0$ and ±1, respectively, and $S_\pm$ are the atomic d states with $m_z=\pm1$. In Eq. (71) about 90% of the contribution comes from the s orbitals, $\cos\theta^{\pm}$ and $\sin\theta^{\pm}$ are the spin-orbit mixing parameters; α and β denote the parameters of a Kramer's pair and the spin states ↑ and ↓ refer to the eigenstates of S_z in a coordinate system with $X=[\bar{1}\bar{1}2]$, $Y=[1\bar{1}0]$, and $Z=[111]$ axes of a valley at one of the L points out of the four in the Brillouin zone. We evaluate the matrix elements of $\sigma^z\mathcal{J}(\vec{r})$ and $\sigma^x\mathcal{J}(\vec{r})$ using these wave functions and these are

$$\langle L_{61}^{+}\alpha(\beta)|\sigma^z\mathcal{J}(r)|L_{61}^{+}\alpha(\beta)\rangle = \pm A\Omega_c, \tag{73}$$

$$\langle L_{62}^{-}\alpha(\beta)|\sigma^z\mathcal{J}(r)|L_{62}^{-}\alpha(\beta)\rangle = \pm B\Omega_c, \tag{74}$$

$$\langle L_{61}^{+}\alpha|\sigma^x\mathcal{J}(r)|L_{61}^{+}\beta\rangle = -a_1\Omega_c \tag{75}$$

and

$$\langle L_{62}^{-}\alpha|\sigma^x\mathcal{J}(r)|L_{62}^{-}\beta\rangle = b_1\Omega_c, \tag{76}$$

where

$$A = a_1 - a_2, \tag{77}$$

$$B = b_1 - b_2, \tag{78}$$

$$a_1 = \cos^2\theta^{+}\langle R|\mathcal{J}(r)|R\rangle/\Omega_c, \tag{79}$$

$$a_2 = \sin^2\theta^{+}\langle S_{+}|\mathcal{J}(r)|S_{+}\rangle/\Omega_c, \tag{80}$$

$$b_1 = \sin^2\theta^{-}\langle z|\mathcal{J}(r)|z\rangle/\Omega_c, \tag{81}$$

and

$$b_2 = \cos^2\theta^{-}\langle X_{+}|\mathcal{J}(r)|X_{+}\rangle/\Omega_c. \tag{82}$$

We briefly describe the calculational procedure below. In PbTe the energy surfaces at the L points are approximately prolate spheroids with the major axes in the [111] directions. Therefore, within the first Brillouin zone there are eight half-spheroids or equivalently four completely spheroidal energy surfaces. However, as discussed earlier, with $\vec{k}$ values away from those at the band edges, the surfaces of constant energy become cylindrical. The momentum, spin and the exchange interaction matrix elements occurring in P_s are evaluated at an arbitrary $\vec{k}$ point by using the wave functions [Eqs. (57)–(60)] and the MW wave functions for the far bands. In the absence of a magnetic field all the four valleys at the ⟨111⟩ zone edges are equivalent. However, in an arbitrarily oriented external magnetic field, neither the matrix elements of $\vec{\sigma}$ nor the Fermi population factors are identical in the four valley at the ⟨111⟩ zone edges. It is convenient to treat the problem of four valleys by evaluating the susceptibility in each of the four symmetrically equivalent coordinate systems ($X_n, Y_n, Z_n, :1-4$) with each Z_n axis along the principal axis of one of the four valleys. Following Mitchell and Wallis we take X_1, Y_1, Z_1 axes along $[\bar{1}\bar{1}2]$, $[1\bar{1}0]$, [111], crystallographic directions, respectively. The remaining three coordinate systems are generated by four fold rotations about the Z axis [001]. Since, when the field is applied in [001] direction, all the four valleys are equivalent, we evaluate P in one valley and multiply by four to account for all valleys.

We can express Z direction in terms of the crystallographic directions as

$$Z = a_{zx_1}X_1 + a_{zy_1}Y_1 + a_{zz_1}Z_1, \tag{83}$$

where $a_{zx_1}=2/\sqrt{3}$, $a_{zy_1}=0$, and $a_{zz_1}=1/\sqrt{3}$. Using the well-known transformation formula, we have

$$P_{js}^{zz} = \sum_{\eta,\lambda=X_1}^{Z_1} a_{z\eta}a_{z\lambda}P_{js}^{\eta\lambda}. \tag{84}$$

Since we are interested in the diagonal components of the EPR shift tensor, Eq. (84) can be written as

$$P_{js}^{zz} = a_{zx_1}^2 P_{js}^{x_1x_1} + a_{zy_1}^2 P_{js}^{y_1y_1} + a_{zz_1}^2 P_{js}^{z_1z_1}. \tag{85}$$

Using the above values of a_{zx_1}, a_{zy_1}, and a_{zz_1}, we have

$$P_{js}^{zz} = \tfrac{1}{3}P_{js}^{z_1z_1} + \tfrac{2}{3}P_{js}^{x_1x_1}. \tag{86}$$

Denoting $P_{js}^{z_1z_1}$ as P_{js}^l and $P_{js}^{x_1x_1}$ as P_s^t, we can write P_{js} as

$$P_{js} = 4\left(\tfrac{1}{3}P_{js}^l + \tfrac{2}{3}P_{js}^t\right), \tag{87}$$

where P_{js}^l and P_{js}^t are the longitudinal and the transverse spin-EPR shifts for any valley. These two quantities are obtained from Eq. (28) and are

TABLE II. Different contributions to P_s^t (all values in units of 10^{-3}) at Mn^{2+} ion in $Pb_{1-x}Mn_xTe$. Both two-band (band-edge) and far-band contributions are considered. Both the contributions are of the same sign, unlike in P_s^l. The fraction of far-band contributions is much smaller, which increases with increase in carrier density.

p (cm^{-3})	P_s^t (two-band)	P_s^t (far-band-inter)	P_s^t (far-band-intra)	P_s^t
5×10^{17}	−0.615	−0.002	−0.016	−0.633
3×10^{18}	−0.570	−0.0029	−0.08	−0.653

$$P_{js}^{l} = -\frac{1}{4}\sum_{n,\vec{k},\rho,\rho',\rho'',m\neq n}\left((\sigma^z\mathcal{J}(r))_{n\rho,n\rho'}\sigma^z_{n\rho',n\rho} + \frac{1}{m}\frac{[\sigma^z\mathcal{J}(r)]_{n\rho.n\rho'}(\pi^-_{n\rho',m\rho''}\pi^+_{m\rho'',n\rho'} - \pi^+_{n\rho',m\rho''}\pi^-_{m\rho'',n\rho})}{E_{mn}}\right)f'(E_{n\vec{k}}) \tag{88}$$

and

$$P_{js}^{t} = -\frac{1}{4}\sum_{n\vec{k},\rho,\rho',m,\rho'',m\neq n}\left((\sigma^x\mathcal{J}(r))_{n\rho,n\rho'}\sigma^x_{n\rho',n\rho} + \frac{1}{\sqrt{2}m}\frac{[\sigma^x\mathcal{J}(r)]_{n\rho,n\rho'}[(\pi^+ - \pi^-)_{n\rho',m\rho''}\pi^z_{m\rho'',n\rho} - \pi^z_{n\rho',m\rho''}(\pi^+ - \pi^-)_{m\rho'',n\rho}]}{E_{mn}}\right)f'(E_{n\vec{k}\rho}), \tag{89}$$

where n stands for the wave functions ϕ_3 and ϕ_4 and m does for ϕ_1, ϕ_2, and other far band basis functions. $E_{n\vec{k}\rho}$ is the total valence band energy. In Eqs. (88) and (89), we have taken $g_j=2$ because for Mn^{2+}, $S=\frac{5}{2}$, and $L=0$. Different matrix elements are evaluated by taking ϕ_1 to ϕ_4 for the band edge states and $L^+_{62}\alpha$, β, $L^+_{5,4}\alpha$, β and $L^-_{61}\alpha$, β and $L^-_{5,4}\alpha$, β of the MW paper[39] for the far bands. The $\vec{k}$ summation was done numerically by considering cylindrical coordinates in the momentum space. The spin-orbit mixing parameters $\sin\theta^{\pm}$ and $\cos\theta^{\pm}$, and the single group energy values are taken from Bernick-Kleinman.[40] The single group momentum matrix elements such as P_{11}, P_{13}, P_{14} for PbTe were obtained through a private communication.[42] The $s(p)$-d exchange parameters a_1, a_2, b_1, b_2, A and B are obtained from Dietl *et al.*[43]

V. RESULTS AND DISCUSSION

Our results for P_s are presented in Tables I–III. We have calculated the anisotropic EPR shift for two typical carrier densities, $p=5\times10^{17}$ cm^{-3} and $p=3.5\times10^{18}$ cm^{-3} in three different ways. Apart from the use of the present electronic structure which gives P_s (new), we have also calculated P_s (old) by using the old method of single diagonalization of band edge states and extending this to include sixth order terms in k_ρ^2 and k_z, which gives the contribution, P_s (old +sixth order).

TABLE III. Results of P_s (all in the units of 10^{-3}) calculated in three different ways and comparison with experiment. P_s (new) is calculated using the modified $\vec{k}\cdot\vec{\pi}$ model in which case the Hamiltonian for band edge states are rediagonalized. P_s (old) represents the model in which the band-edge states are diagonalized only once and energy is expanded up to k^4 terms. P_s (old+sixth order) follows the old method except that the total energy expression is expanded up to k^6 terms. However, inclusion of extra terms does not improve the old results for the carrier densities considered. The new model gives better agreement with the experimental results.

p (cm^{-3})	P_s (new)	P_s (old+sixth order)	P_s (old)	P_s (expt.)
5×10^{17}	−3.69	−5.14	−5.14	−3.14
3.5×10^{18}	−2.98	−4.98	−4.98	−2.00

From Table III, we see that the present model gives better results vis-a-vis experimental results,[4] justifying its better accuracy. In Tables I and II, we present the longitudinal (P_s^l) and transverse (P_s^t) contributions to P_s. It is observed that there is considerable anisotropy. Each of these contributions is expressed as a sum of a two-band contribution P_s^ϵ (two-band), P_s^ϵ (far band-inter) which takes into account the interaction of the valence band with the other two conduction bands and P_s^ϵ (far band-intra) which considers the interaction of the valence band edge with the other two valence bands. Here ϵ stands for l and t. In both cases we see that the two-band contributions are dominant. While in the longitudinal shift, the far-band-intra contribution is smaller than the far-band-inter contribution, the reverse thing happens in case of P_s^t. While in case of P_s^l, the far band contributions have opposite sign with regard to the band-edge contributions, in case of P_s^t, all the three contributions have the same sign, for both the carrier densities. In case of P_s^l, (Table I) the far band contributions together account for a significant fraction of the dominant two band contribution, which increases with increase in the carrier density. On the other hand, for P_s^t (Table II) the far band interactions together constitute a very small fraction of the two-band contributions. However, as in P_s^l, this fraction increases with increase in the carrier density.

There is considerable anisotropy, as expected, due to the large spin-orbit interaction which contributes to the anisotropy of the g factor. The anisotropy could also result from *sp-d* hybridization,[25] but we have not considered it here. Further, the two band or band-edge contributions are dominant, as expected, because of the smaller energy gap between the band edge states. Another mechanism which we have not considered is the contribution due to the core polarization which is an intra-atomic phenomenon. However, we cannot comment on its possible strength without a quantitative analysis for the Mn^{2+} ion.

Now we wish to comment on the higher theoretical values obtained in comparison with the experimental values. While the values obtained in the new model are slightly higher than the experimental values, those obtained following the old method are considerably higher. The old model gives larger Fermi energies owing to the inadequate treatment of interband interactions in the $\vec{k}\cdot\vec{\pi}$ method. Because of the narrow gaps in these semiconductors, departure from the linear behavior occurs for small concentrations and this is not reflected in our old model. The slightly higher new values may be due presumably to the core polarization and other mechanisms we have not considered.

In conclusion, we wish to state that we present in this work a reasonably detailed theory of the spin-EPR shift in $Pb_{1-x}Mn_xTe$. There is a good agreement with experimental results for the two typical carrier densities considered. Notwithstanding the encouraging results, there is still scope for improvement. In deriving P_s, we have neglected some terms which should have given some additional contributions owing to the spin-orbit interactions alone, in addition to the term retained which modifies the carrier g factor. There could be some contribution from the interaction of the magnetic ions mediated by carriers (RKKY) which is oscillatory in nature. However, this contribution is not expected to be significant since RKKY interaction results from second-order effects. In spite of the omission of these possibly useful mechanisms, we see that our results agree fairly well with the experimental results.

ACKNOWLEDGMENT

The research was supported partly by the UGC, India.

---

*Electronic address: gs_tripathi@hotmail.com

[1] W. D. Knight, Phys. Rev. **76**, 1259 (1949).

[2] C. H. Townes, C. Herring, and W. D. Knight, Phys. Rev. **77**, 852 (1950).

[3] C. P. Slichter, *Principles of Magnetic Resonance* (Harper and Row, New York, 1963).

[4] T. Story, C. H. W. Swuste, P. J. T. Eggenkamp, H. J. M. Swagten, and W. J. M. de Jonge, Phys. Rev. Lett. **77**, 2802 (1996).

[5] G. S. Tripathi, L. K. Das, P. K. Misra, and S. D. Mahanti, Solid State Commun. **38**, 1207 (1981); Phys. Rev. B **25**, 3091 (1982).

[6] R. L. Hota and G. S. Tripathi, Phys. Rev. B **44**, 1918 (1991).

[7] R. L. Hota, C. M. Misra, and G. S. Tripathi, Phys. Rev. B **45**, 10783 (1992).

[8] G. S. Tripathi, C. M. Misra, and P. K. Misra, J. Phys. C **18**, L935 (1985).

[9] R. L. Hota, R. C. Patnaik, G. S. Tripathi, and P. K. Misra, Phys. Rev. B **51**, 7291 (1995).

[10] G. S. Tripathi, Phys. Rev. B **31**, 5143 (1985).

[11] R. C. Patnaik, R. L. Hota, and G. S. Tripathi, Phys. Rev. B **58**, 3924 (1998).

[12] R. L. Hota, G. S. Tripathi, and J. N. Mohanty, Phys. Rev. B **47**, 9319 (1993).

[13] R. L. Hota, G. S. Tripathi, and P. K. Misra, J. Appl. Phys. **75**, 5737 (1994).

[14] R. K. Das and G. S. Tripathi, J. Phys. Chem. Solids **64**, 993 (2003).

[15] H. Ohno, Science **291**, 840 (2001).

[16] H. Ohno, Science **281**, 951 (1998).

[17] K. Sato and H. Katayama-Yoshida, Semicond. Sci. Technol. **17**, 367 (2002).

[18] T. Dietl, H. Ohno., and E. Matsukura, Phys. Rev. B **63**, 195205 (2001).

[19] R. Akimoto, K. Ando, F. Sasaki, S. Kobayashi, and T. Tani, Phys. Rev. B **57**, 7208 (1998).

[20] M. Berciu and R. N. Bhatt, Phys. Rev. B **69**, 045202 (2004).

[21] S. Koshihara, A. Oiwa, M. Hirasawa, S. Katsumoto, Y. Iye, C. Urano, H. Takagi, and H. Munekata, Phys. Rev. Lett. **78**, 4617 (1997).

[22] R. R. Galazka, J. Magn. Magn. Mater. **140–144**, 13 (1995).

[23] C. W. H. M. Vennix, E. Frikkee, P. J. T. Eggenkamp, H. J. M. Swagten, K. Kopinga, and W. J. M. de Jonge, Phys. Rev. B **48**, 3770 (1993).

[24] P. J. T. Eggenkamp, H. J. M. Swagten, T. Story, V. I. Litvinov, C. H. W. Swuste, and W. J. M. de Jonge, Phys. Rev. B **51**, 15250 (1995).

[25] R. C. Patnaik and G. S. Tripathi, Solid State Commun. **112**, 669 (1999).

[26] P. K. Misra and L. M. Roth, Phys. Rev. **177**, 1089 (1969).

[27] P. K. Misra and L. Kleinman, Phys. Rev. B **5**, 4581 (1972).

[28] S. K. Misra, P. K. Misra, and S. D. Mahanti, Phys. Rev. B **26**, 1903 (1982).

[29] J. M. Luttinger and W. Kohn, Phys. Rev. **97**, 869 (1955).

[30] E. O. Kane, J. Phys. Chem. Solids **1**, 249 (1957).

[31] J. M. Luttinger and J. C. Ward, Phys. Rev. **118**, 1417 (1960).

[32] Y. A. Bychov and L. P. Gorkov, Zh. Eksp. Teor. Fiz. **41**, 1592 (1961) [Sov. Phys. JETP **14**, 1132 (1962)].

[33] F. A. Buot, Phys. Rev. B **14**, 3310 (1976).

[34] M. A. Phillippas and J. W. McClure, Phys. Rev. B **6**, 2051 (1972).

[35] R. Peierls, Z. Phys. **80**, 763 (1933).

[36] A. Trellakis, Phys. Rev. Lett. **91**, 056405 (2003).

[37] A. S. Alexandrov and H. Capellmann, Phys. Rev. Lett. **66**, 365 (1991).

[38] R. K. Das, S. Sahoo, and G. S. Tripathi, Semicond. Sci. Technol. **19**, 433 (2004).

[39] D. L. Mitchell and R. F. Wallis, Phys. Rev. **151**, 581 (1966).

[40] R. L. Bernick and L. Kleinman, Solid State Commun. **8**, 569 (1970).

[41] G. Bauer and H. Pascher, in *Semi-Magnetic Semiconductors and Dilute Magnetic Semiconductors*, edited by M. Averous and M. Balkanski (Plenum, New York, 1991).

[42] L. Kleinman (private communication).

[43] T. Dietl, C. Silwa, G. Bauer, and H. Pascher, Phys. Rev. B **49**, 2230 (1994).